Research Square

Preprints are preliminary reports that have not undergone peer review.
They should not be considered conclusive, used to inform clinical practice,
or referenced by the media as validated information.

Spatially-explicit modeling of multi-hazard exposure in mountain ecosystems: Unraveling the role of canopy structure in forest vulnerability

Davood Mafi-Gholami
Standard Research Institute
Abolfazl Jaafari
Agricultural Research, Education and Extension11 Organization (AREEO)
Binh Thai Pham
binhpt@utt.edu.vn

University of Transport Technology

Research Article

Keywords: Exposure, Spatial Modeling, Zagros Forests, Vulnerability.

Posted Date: July 13th, 2026

DOI: https://doi.org/10.21203/rs.3.rs-10110474/v1

License: This work is licensed under a Creative Commons Attribution 4.0 International License.
Read Full License

Additional Declarations: No competing interests reported.

Version of Record: A version of this preprint was published at Environmental Monitoring and Assessment on September 1st, 2026. See the published version at https://doi.org/10.1007/s10661-026-15874-1.

Spatially-explicit modeling of multi-hazard exposure in mountain ecosystems: Unraveling the role of canopy structure in forest vulnerability

Davood Mafi-Gholami[1], Abolfazl Jaafari[2], Binh Thai Pham[3*]

1. Management Systems Research Group, Quality Assessment and Management Systems Research Center, Standard Research Institute, Karaj 31585-163, Iran. Email: d.mafi@standard.ac.ir

2. Research Institute of Forests and Rangelands, Agricultural Research, Education and Extension11 Organization (AREEO), Tehran, 1496813111, Iran. Email: jaafari@rifr-ac.ir

3. Intelligent Geosystems and Infrastructure Research Group, University of Transport Technology, 54 Trieu Khuc, Thanh Liet, Hanoi 100000, Vietnam, binhpt@utt.edu.vn

* Corresponding author

Abstract

Mountain forests are increasingly threatened by interacting climatic, environmental, and socio-ecological stressors, yet most vulnerability assessments continue to rely on single-hazard approaches that fail to capture the cumulative nature of environmental risk. This limitation is particularly pronounced in the Zagros forests of Iran, one of the largest and most ecologically significant dry forest ecosystems in the Middle East, where climate change and human-induced pressures are accelerating forest degradation. This study developed a spatially explicit multi-hazard exposure framework to quantify forest exposure to multiple environmental hazards and to examine its relationship with forest canopy-cover structure. Nine environmental and socio-ecological hazards, including drought, actual evapotranspiration, wildfire, high-speed winds, maximum temperature, floods, landslides, dust storms, and social vulnerability, were integrated within a GIS-based multi-criteria framework using expert-derived weights obtained through the Delphi method. Following standardization, all hazard layers were harmonized to a common spatial resolution of 30 m and combined to produce a high-resolution exposure index across the forest landscapes. Model performance was independently validated using 448 disturbance records comprising oak decline locations, field-observed forest degradation sites, and documented wildfire hotspots. The results revealed pronounced spatial heterogeneity in exposure patterns, with more than half of the forest area classified within high and very high exposure categories. Drought emerged as the dominant hazard, followed by wildfire and social vulnerability, highlighting the combined influence of climatic and socio-ecological pressures on forest risk. Exposure intensity increased consistently with declining canopy cover, and sparsely forested stands

exhibited the greatest concentration and spatial continuity of high-risk zones. Independent validation demonstrated strong model reliability, with 75% of disturbance records located within high and very high exposure classes. These findings identify forest canopy structure as a critical regulator of multi-hazard exposure and provide a robust decision-support framework for forest restoration, climate adaptation, risk management, and conservation planning in climate-sensitive mountain forest ecosystems worldwide.
Keywords: Exposure, Spatial Modeling, Zagros Forests, Vulnerability.

1. Introduction

Forests constitute one of the fundamental components of the Earth's biosphere, covering approximately 4.6 billion hectares and accounting for nearly one-third of the global land surface. They represent the primary reservoir of terrestrial biodiversity, harboring more than 80% of the world's plant, animal, and insect species (FAO, 2020). In addition to their ecological significance, forests play a pivotal role in climate regulation by storing nearly 78% of the organic carbon contained within terrestrial ecosystems and acting as one of the largest global carbon sinks through carbon sequestration and storage. From a socio-economic perspective, forests provide essential goods and ecosystem services that support the livelihoods of a substantial proportion of the global population. Approximately one-quarter of the world's population depends directly or indirectly on forest resources, while a similar proportion of household income in developing countries is derived from forest-related products and services (FAO, 2020).

Despite these critical functions, forest ecosystems have increasingly been exposed to multiple and interacting environmental stressors over recent decades. These stressors encompass a wide range of climatic and anthropogenic drivers, including rising temperatures, recurrent drought events, dust storms, pest and disease outbreaks, unsustainable resource exploitation, land-use change, overgrazing, wildfires, and flooding (Leberger et al., 2020). The interaction among these hazards has intensified ecosystem degradation processes and shifted forest risk assessments from single-hazard approaches toward more comprehensive multi-dimensional frameworks.

Among forest ecosystems, mountain forests are considered particularly vulnerable due to their unique ecological characteristics and heightened sensitivity to environmental change. These forests account for approximately 25% of the world's forested area and provide critical ecosystem services and livelihood support for more than 900 million people worldwide (Spehn et al., 2011). Nevertheless, mountain forests are increasingly subjected to a combination of climate-related pressures, anthropogenic disturbances, land-use and land-cover changes, pollution, and biological threats such as pests and diseases (Thakur et al., 2021). The cumulative impacts of these pressures have resulted in profound alterations in forest structure and dynamics, including declines in productivity, shifts in fire regimes, increased pest outbreaks, species redistribution, and biodiversity loss (Liu et al., 2013; Valavi et al., 2019).

In response to these challenges, numerous studies have investigated forest degradation and vulnerability at regional and national scales. For example, Michelsen et al. (2014) examined the impacts of land-use change and forestry activities on biodiversity in Norway, emphasizing the ecological consequences of human interventions. Liu et al. (2013) demonstrated that increasing temperatures and intensified climatic aridity can substantially reduce tree growth and ecosystem stability in semi-arid forests of China. Similarly, Valavi et al. (2019) modeled the effects of climate change on the distribution and persistence of Zagros forest ecosystems in Iran and reported increasing vulnerability under future climate scenarios. Collectively, these studies highlight the significant influence of climatic and environmental stressors on forest ecosystem functioning. However, integrated assessments of exposure to multiple environmental hazards remain relatively scarce in the Zagros forests.

Although considerable progress has been made in understanding the impacts of climate change, drought, wildfire, land-use change, and other environmental stressors on forest ecosystems, previous studies in the Zagros region have largely focused on individual hazards or on the effects of a limited number of environmental drivers. In reality, these ecosystems are simultaneously exposed to multiple climatic, environmental, and anthropogenic hazards whose complex interactions shape degradation processes and ecosystem instability. Consequently, single-hazard approaches are insufficient to capture the complexity of these interactions, highlighting the need for integrated frameworks capable of assessing exposure to multiple environmental hazards.

Furthermore, while various studies have investigated different environmental threats within the Zagros forests, limited attention has been given to the integrated assessment of the exposure component of vulnerability and its relationship with forest structural characteristics, particularly canopy cover density. This is despite the fact that canopy structure represents one of the most important determinants of forest ecological stability and may significantly influence the extent to which forests are affected by environmental hazards.

These considerations underscore the necessity of improving our understanding of forest vulnerability and its underlying drivers to support sustainable management and conservation of the Zagros forests. Within vulnerability assessment frameworks, vulnerability is commonly conceptualized as a function of three interrelated components: exposure, sensitivity, and adaptive capacity (Mafi-Gholami et al., 2021). Among these, exposure refers to the magnitude, intensity, spatial extent, and duration of a system's contact with environmental disturbances and stressors (Adger, 2006). As the initial component of vulnerability assessment, exposure plays a fundamental role in identifying critical areas and characterizing the spatial distribution of multiple hazards. Therefore, the identification, quantification, and spatial modeling of environmental hazards constitute essential steps toward developing effective management strategies, prioritizing conservation actions, and enhancing ecosystem resilience.

In this context, the present study addresses an important knowledge gap by integrating nine environmental and socio-ecological hazards to model the spatial distribution of the exposure component and to investigate its relationship with forest canopy structure. By doing so, the study seeks to advance current understanding of multi-hazard exposure in the Zagros forests and provide a scientific basis for risk-informed management and long-term ecosystem conservation.

At the national scale, the Zagros mountain forests cover approximately 5 million hectares and constitute nearly 40% of Iran's total forest area. Located within a semi-Mediterranean climatic zone, these forests play a crucial role in hydrological regulation, soil conservation, climate moderation, and the maintenance of regional socio-economic systems (Pourhashemi et al., 2004). However, during recent decades, these ecosystems have experienced increasing pressure from both natural and anthropogenic threats, including declining precipitation, intensified drought, rising temperatures, dust storms, pest and disease outbreaks, unsustainable exploitation, overgrazing, and recurrent wildfires, all of which have contributed to the degradation of forest extent and quality (Pouyan et al., 2021).

Under such circumstances, the development of advanced analytical approaches and decision-support tools is essential for effective forest conservation. Achieving this objective requires robust assessments of ecosystem vulnerability, particularly the exposure component to multiple environmental hazards. Spatial identification and modeling of hazard intensity and distribution can provide valuable information for designing targeted management strategies and enhancing forest resilience.

Accordingly, this study seeks to address the following research questions: (1) What is the spatial pattern of exposure to multiple environmental hazards across forest ecosystems in Kohgiluyeh and Boyer-Ahmad Province? (2) Which environmental hazards exert the greatest influence on the spatial distribution of exposure across forest landscapes? and (3) How is exposure to multiple environmental hazards related to different classes of forest canopy cover density?

To answer these questions, the primary objective of this study is to spatially model exposure to multiple environmental hazards in the Zagros forests and to examine its relationship with forest canopy structure in Kohgiluyeh and Boyer-Ahmad Province, southwestern Iran.

2. Materials and methods

2.1. Study area

Kohgiluyeh and Boyer-Ahmad Province, covering approximately 15,500 km², is located in southwestern Iran within the central Zagros Mountain range and represents one of the country's most prominent mountainous regions. Geographically, the province extends between approximately 30°09′–31°32′ N latitude and 49°57′–51°42′ E longitude (Fig. 1). Owing to its complex geomorphological setting, the region exhibits substantial spatial heterogeneity in elevation, slope gradient, and aspect, resulting in diverse

environmental and ecological conditions across the landscape. These forests are predominantly composed of Persian oak (*Quercus brantii*), which constitutes the dominant tree species and forms one of the most ecologically valuable forest ecosystems in western Iran. Beyond their biodiversity significance, these forests provide a wide range of ecosystem services, including carbon sequestration, soil conservation, watershed protection, climate regulation, and support for local livelihoods and regional socio-economic systems.

Despite their ecological importance, the forests of Kohgiluyeh and Boyer-Ahmad Province have experienced increasing environmental pressures during recent decades. These pressures arise from the combined effects of anthropogenic disturbances and climate-related stressors. Major human-induced drivers include unsustainable forest exploitation, excessive livestock grazing, land-use and land-cover changes, and infrastructure development with limited environmental considerations. Simultaneously, the region has been increasingly affected by climate variability and the growing frequency and intensity of extreme environmental events, including prolonged droughts, rising temperatures, and recurrent forest fires (Pouyan et al., 2021).

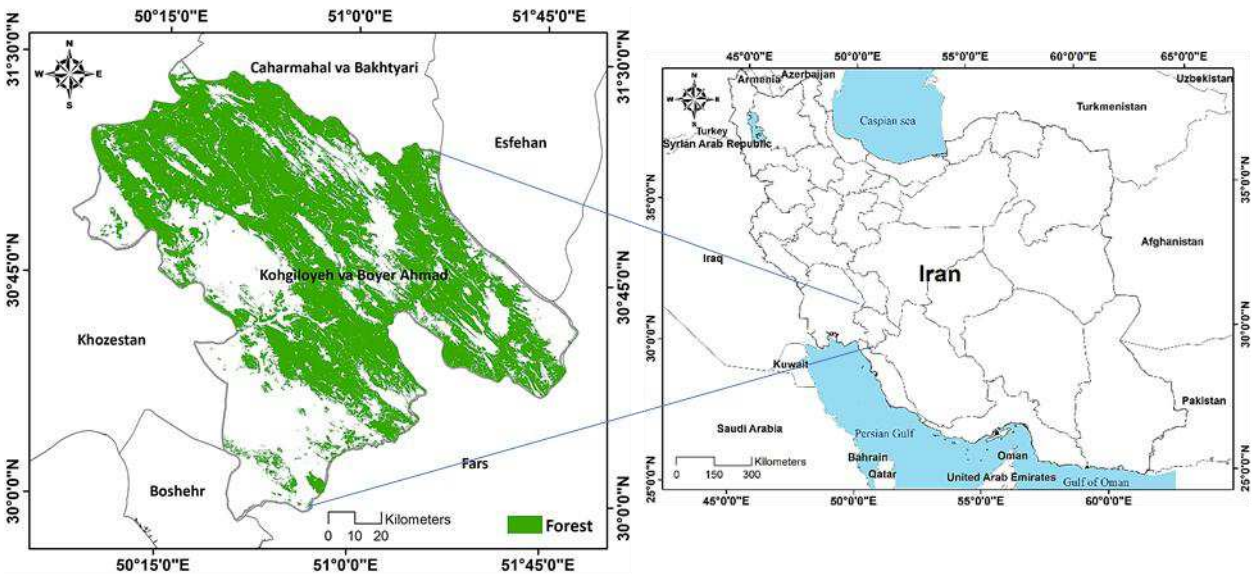


Fig. 1. Geographic location of the study area and spatial distribution of forest ecosystems in Kohgiluyeh and Boyer-Ahmad Province, southwestern Iran

2.2. Spatial modeling of the exposure index

To quantify the exposure component of forest vulnerability, nine environmental and socio-ecological hazards were incorporated into the analysis, including drought, high-speed winds, maximum temperature, social vulnerability, dust storms, actual evapotranspiration, flood, wildfire, and landslide occurrence. These hazards were selected based on an extensive review of previous studies addressing environmental threats to

159 forest ecosystems (Eslami-Andargoli et al., 2009; Ellison, 2000; Macek et al., 2019; Xiao et al., 2013;
160 Donmez & Berberoglu, 2016; Mafi-Gholami et al., 2019, 2021), analysis of available environmental reports
161 and datasets, field observations, and the availability of reliable spatial information for hazard mapping
162 within the study area.
163 Given the heterogeneous nature of the selected hazard indicators and their differing measurement scales, all
164 hazard layers were standardized prior to integration. To facilitate comparability among variables and ensure
165 consistency within the multi-hazard assessment framework, each hazard map was classified into four ordinal
166 categories representing low, moderate, high, and very high hazard intensity. Classification thresholds were
167 determined independently for each hazard layer using the Natural Breaks (Jenks) classification method in
168 ArcGIS. This approach identifies natural groupings within the data by maximizing variance between classes
169 while minimizing variance within classes, and is widely employed in environmental hazard assessment and
170 spatial risk analysis. Consequently, class boundaries were established according to the statistical
171 characteristics and spatial distribution patterns of each variable.
172 Because the datasets utilized in this study originated from multiple sources with different spatial resolutions
173 and formats, a comprehensive preprocessing procedure was implemented prior to spatial integration. All
174 datasets were transformed into a common coordinate reference system, spatial extent, and raster framework.
175 Hazard layers derived from MODIS satellite products, meteorological station observations, digital elevation
176 models, natural hazard datasets, and socio-economic indicators were converted to raster format and
177 resampled to a common spatial resolution of 30 × 30 m. The selection of a 30-m spatial resolution was
178 motivated by the need to adequately capture the spatial heterogeneity of the Zagros forest ecosystems while
179 maintaining compatibility with the environmental and topographic datasets used in the analysis. Following
180 standardization and resampling, all spatial analyses, weighting procedures, and overlay operations were
181 conducted within a unified raster environment based on a 30 × 30 m grid structure. This procedure ensured
182 spatial consistency among datasets and minimized potential uncertainties arising from differences in the
183 original spatial resolutions of the input layers. The final exposure index was generated through the weighted
184 integration of the nine hazard layers, producing a spatially explicit representation of the degree to which
185 forest ecosystems are exposed to multiple environmental hazards across the study area.
186
187 **2.3. Hazard identification and selection**
188 The identification and selection of environmental hazards incorporated into the exposure assessment
189 framework were based on a comprehensive and multi-source evaluation process. Four principal sources of
190 information were employed: (1) an extensive review of the scientific literature addressing the impacts of
191 environmental hazards on forest ecosystem structure, functioning, and resilience; (2) technical reports,
192 environmental assessments, and official documents related to the ecological condition and degradation

processes of the Zagros forests; (3) field observations and site inspections conducted within the study area; and (4) the availability of reliable spatial datasets suitable for hazard mapping and geospatial analysis.

Previous studies have demonstrated that forest ecosystems are increasingly affected by a wide range of interacting environmental stressors, including drought, thermal extremes, altered fire regimes, flooding, landslides, strong winds, dust storms, and socio-environmental pressures. These hazards can directly or indirectly influence forest health, ecological stability, regeneration capacity, biodiversity conservation, and ecosystem functioning (Ellison, 2000; Eslami-Andargoli et al., 2009; Xiao et al., 2013; Donmez & Berberoglu, 2016; Macek et al., 2019; Mafi-Gholami et al., 2019, 2021; Haidari et al., 2025). Given the complex interactions among these drivers, evaluating exposure through a multi-hazard framework is essential for understanding the spatial patterns of forest vulnerability.

The final selection of hazards was guided by three criteria: (i) documented ecological relevance and demonstrated impacts on forest ecosystems, particularly within the Zagros region; (ii) representativeness of the dominant climatic, environmental, geomorphological, and socio-ecological stressors affecting the study area; and (iii) availability of spatially explicit and scientifically reliable datasets for regional-scale modeling. Based on these criteria, nine hazards were identified as the most influential drivers of forest exposure and were subsequently incorporated into the analysis: drought, actual evapotranspiration, wildfire, high-speed winds, maximum temperature, flooding, landslides, dust storms, and social vulnerability. These hazards collectively capture the major climatic, ecological, geomorphological, and socio-environmental pressures currently affecting the Zagros mountain forests. Accordingly, they were used to construct the spatial Exposure Index and to characterize the degree of environmental hazard exposure across forest ecosystems within the study area.

2.3.1. Mapping of high-speed wind hazard

The spatial distribution of high-speed wind hazard across the study area was assessed by focusing on wind speeds equal to or exceeding 10.8 m s^{-1}, corresponding to the onset of Beaufort Scale Force 6. This threshold was selected because sustained winds of this magnitude can exert significant ecological stress on forest ecosystems through increased mechanical damage, canopy disturbance, stem breakage, reduced tree stability, and enhanced susceptibility to secondary disturbances. To characterize the temporal and spatial occurrence of high-wind events, a long-term dataset of three-hourly wind speed observations covering the period 1990–2025 was obtained from 12 synoptic meteorological stations located within and surrounding the forested areas of the study region. The use of a 36-year observation period provided a robust representation of regional wind climatology and enabled the assessment of long-term hazard patterns.

To model the statistical behavior of wind speed and estimate the probability of occurrence of different wind-speed classes, the Weibull probability distribution function was employed. Owing to its flexibility and

proven ability to accurately represent wind speed frequency distributions, the Weibull distribution is widely used in climatological and wind-hazard studies (Li et al., 2025). The Weibull probability density function applied in this study is expressed as follows:

$$f(v) = \left(\frac{k}{c}\right)\left(\frac{k}{c}\right)^{k-1} \exp\left[-\left(\frac{k}{c}\right)^{k}\right] \qquad (k > 0, v > 0, c > 1) \qquad (1)$$

where v is the wind speed in ms^{-1}, f(v) is the probability of occurrence for a specific wind speed in ms^{-1}, k is the shape factor (dimensionless), and c is the Weibull scale factor in ms^{-1}.

For each meteorological station, the estimated probability of occurrence was combined with the mean wind speed exceeding the selected threshold of 10.8 m s^{-1} to derive a quantitative high-wind hazard index. This procedure enabled the integration of both wind intensity and occurrence probability into a single hazard metric. Subsequently, the station-based hazard values were spatially interpolated using the Inverse Distance Weighting (IDW) method within the ArcGIS environment to generate a continuous raster surface of high-wind hazard across the study area. The IDW technique was selected because of its effectiveness in representing spatially continuous environmental variables from irregularly distributed observation stations and its widespread application in climatological and environmental mapping studies (Mafi-Gholami et al., 2021). Finally, the resulting hazard map was classified into four ordinal hazard classes, namely low, moderate, high, and very high, using the Natural Breaks (Jenks) classification method. This classification facilitated subsequent integration with other environmental hazard layers and enabled consistent interpretation of the relative spatial intensity of high-wind hazard across the forest ecosystems of the study area.

2.3.2. Drought hazard mapping

Drought hazard was assessed using long-term precipitation records obtained from 12 synoptic meteorological stations located within and around the forest ecosystems of the study area. The dataset covered a continuous 36-year period (1990–2025), providing a robust basis for characterizing the temporal variability and spatial distribution of meteorological drought across the Zagros forests.

To quantify drought conditions, the Standardized Precipitation Index (SPI) was employed at the annual time scale. SPI is one of the most widely used drought indicators because it standardizes precipitation anomalies and enables consistent comparison of drought severity across regions with different climatic characteristics (Mafi-Gholami et al., 2021). In addition to identifying drought occurrence, SPI effectively captures deviations from long-term precipitation regimes that may influence ecosystem functioning, vegetation health, and forest resilience. Following the calculation of annual SPI values for each meteorological station, drought hazard was characterized using the drought magnitude index, which integrates both the severity and

persistence of drought conditions over the study period. This index was calculated as the cumulative sum of all negative SPI values according to Eq. 2 (Mafi-Gholami et al., 2021):

$$\text{MeteorologicalDrought Magnitude} = -(\sum_{j=1}^{x} \text{SPI}_j) \quad (2)$$

where SPI_jrepresents the negative values of the Standardized Precipitation Index during period j, and $x$denotes the total number of drought periods.

After calculating drought magnitude values for each station, spatial interpolation was performed using the Inverse Distance Weighting (IDW) method in ArcGIS to generate a continuous raster map of drought hazard across the study area. The IDW technique was selected because of its proven effectiveness in representing spatial gradients of climatological variables derived from irregularly distributed meteorological stations (Mafi-Gholami et al., 2021). Finally, the resulting drought hazard layer was classified into four ordinal categories—low, moderate, high, and very high—using the Natural Breaks (Jenks) classification method. This classification facilitated subsequent integration with other environmental hazard layers within the multi-hazard exposure assessment framework and enabled a consistent representation of drought hazard intensity throughout the study area.

2.3.3. Social vulnerability mapping

To develop the Social Vulnerability Index (SoVI) at the rural district level across Kohgiluyeh and Boyer-Ahmad Province, a set of 25 socio-economic indicators and six environmental hazards were selected based on four criteria: (i) a comprehensive review of international social vulnerability studies (Koks et al., 2015; Su et al., 2015; Reckien, 2018; Nguyen et al., 2019; Mafi-Gholami et al., 2021), (ii) the socio-economic characteristics of the study area, (iii) data availability, and (iv) access to reliable statistical information from the Statistical Center of Iran. The selected indicators were organized within three dimensions of vulnerability, namely Exposure, Sensitivity, and Adaptive Capacity (Table 1). A detailed description of the SoVI development procedure can be found in Mafi-Gholami et al. (2021).

The assessment framework adopted in this study follows the widely accepted conceptual model of vulnerability, which considers vulnerability as the result of interactions among three fundamental components: exposure, sensitivity, and adaptive capacity (Turner et al., 2003; Adger, 2006; Cutter et al., 2008; IPCC, 2022). Within this framework, exposure represents the degree to which a system is subjected to external hazards and environmental stresses. Sensitivity refers to the intrinsic demographic and socio-economic characteristics that influence the susceptibility of communities to adverse impacts. Adaptive capacity reflects the economic, institutional, infrastructural, and human resources available to cope with disturbances, reduce potential impacts, adapt to changing conditions, and recover following hazardous events.

Accordingly, the indicators used in this study were classified based on their functional role in the vulnerability formation process. Environmental hazards were considered exposure variables, demographic and social characteristics were treated as sensitivity indicators, and economic, institutional, infrastructural, and human-capital variables were incorporated as adaptive-capacity indicators. Following the calculation of SoVI values for all rural districts, the resulting index was classified into four vulnerability classes (low, moderate, high, and very high) to facilitate spatial interpretation and subsequent integration into the exposure assessment framework.

Table 1. Conceptual framework and indicator structure used for the assessment of social vulnerability across forested rural districts

Subsystem	Vulnerability Component	Sub-dimension	Indicator
Human–Social System	**Exposure**	Environmental Hazards	Maximum temperature
			Dust storms
			Drought
			High winds
			Landslides
			Floods
Human–Social System	**Sensitivity**	Demographic Characteristics	Percentage of population aged >65 years
			Percentage of population aged <5 years
			Percentage of females in the population
			Percentage of female-headed households
			Average household size
			Population density
			Total population
	Social Characteristics	Illiteracy rate	
			Percentage of households with illiterate heads
			Unemployment rate
			Percentage of households with unemployed heads
	Livelihood Dependence	Percentage of agricultural land area	
			Average livestock ownership per household
Human–Social System	**Adaptive Capacity**	Economic Capacity	Average monthly household income

		Average monthly household expenditure
Institutional Capacity	Percentage of population covered by insurance	
		Percentage of households supported by welfare and relief organizations
Infrastructure and Housing Capacity	Percentage of houses with concrete or steel structures	
		Road density (km km^{-2})
Energy Access Capacity	Percentage of households without wood-burning heaters	
		Percentage of households without wood-fired water heaters
Human Capital	Literacy rate	
		Employment rate
		Mean population age

303

304 **2.3.4. Dust hazard mapping**

305 To characterize the spatiotemporal dynamics of dust activity across the studied forest ecosystems, remotely
306 sensed aerosol data derived from the MODIS MCD19A2 Version 6 product onboard the Terra satellite were
307 utilized. Aerosol optical depth (AOD), a widely recognized proxy for atmospheric particulate matter
308 concentration, was extracted and processed within the Google Earth Engine (GEE) cloud-computing
309 platform. Daily AOD observations covering a 22-year period (2002–2024) were first retrieved and organized
310 in the GEE environment. To reduce short-term variability and enhance the detection of dominant temporal
311 patterns, the dataset was aggregated at multiple temporal scales. Monthly mean AOD values were initially
312 calculated and subsequently averaged to generate annual composites, providing a robust representation of
313 long-term dust activity across the study area. For spatial hazard assessment, a dust hazard map was generated
314 based on the spatial distribution of long-term AOD values within the forest landscapes. The resulting AOD
315 surface was classified into four hazard categories (low, moderate, high, and very high) according to the
316 distribution of observed values, enabling the identification of areas with differing levels of exposure to
317 atmospheric dust pollution.

318

319 **2.3.5. Maximum temperature hazard mapping**

320 To assess the spatial distribution of extreme temperature hazard across the forest ecosystems, daily
321 temperature records from 12 synoptic stations located within and around the study area were analyzed for
322 the period 1990–2025. Summer maximum temperatures were extracted for each year to focus on periods of
323 peak thermal stress. For each station, temporal trends in annual maximum temperature were quantified using
324 linear regression, with the regression slope representing the rate of temperature change over time. To

integrate both thermal intensity and long-term warming trends, the mean annual maximum temperature was multiplied by the corresponding rate of change, generating a composite indicator of maximum temperature hazard for each station. The resulting hazard values were spatially interpolated using the Inverse Distance Weighting (IDW) method in ArcGIS to produce a continuous raster surface representing the spatial distribution of thermal hazard across the study area. Finally, the hazard map was classified into four categories (low, moderate, high, and very high) to facilitate spatial comparison and identify areas experiencing different levels of exposure to increasing thermal stress.

2.3.6. Actual evapotranspiration hazard mapping

To characterize the spatial variability of evapotranspiration-related environmental stress across the forest ecosystems, annual potential evapotranspiration (PET) was first estimated for 12 synoptic stations located within and surrounding the study area using the CropWat model. PET values were used as an indicator of atmospheric evaporative demand and served as the basis for subsequent analyses.

Actual evapotranspiration (AET) was then estimated by integrating annual precipitation and PET through a nonlinear empirical model that accounts for moisture limitations under varying climatic conditions (Eq. 3) (Abdollahi et al., 2017).

$$AET = \frac{P}{(\alpha+(\frac{P}{PET})^{\beta})^{\frac{1}{\beta}}} \quad (3)$$

where P is annual precipitation, PET is annual potential evapotranspiration, and α (= 0.9) and β (= 2) are empirical model parameters that account for climatic controls on the estimation of actual evapotranspiration (AET).

This approach provides a realistic representation of water availability constraints on ecosystem evapotranspiration processes.

Following the calculation of AET for each station, the resulting values were spatially interpolated using the Inverse Distance Weighting (IDW) method in ArcGIS to generate a continuous raster surface representing the spatial distribution of evapotranspiration conditions across the study area. Finally, the AET layer was classified into four categories (low, moderate, high, and very high) to facilitate spatial comparison and identify areas experiencing different levels of evapotranspiration-related environmental stress.

2.3.7. Wildfire, landslide, and flood hazard mapping

Spatial datasets representing secondary environmental hazards, including wildfire, landslide, and flood susceptibility, were compiled from previously validated regional hazard assessments. Specifically, wildfire, landslide, and flood hazard maps were derived from the studies of Jaafari (2024), Ngo et al. (2021), and Khosravi et al. (2020), respectively. These datasets were selected due to their demonstrated reliability and

applicability for large-scale environmental risk assessment. To ensure spatial consistency with the study domain, all hazard layers were geospatially harmonized and clipped using the forest ecosystem boundaries, thereby restricting analyses to the targeted forest landscapes. This procedure eliminated extraneous spatial information and improved the accuracy of hazard characterization within the study area. To facilitate comparative assessment and integration of multiple hazard dimensions, each raster layer was standardized and reclassified into four hazard intensity categories (low, moderate, high, and very high) based on the distribution of hazard values. The resulting harmonized hazard maps provided a consistent spatial framework for evaluating the exposure of forest ecosystems to secondary environmental disturbances and for subsequent resilience and vulnerability analyses.

2.4. Hazard weighting through expert-based Delphi assessment

To quantify the relative contribution of environmental hazards within the resilience assessment framework, a Delphi-based expert elicitation approach was employed. A panel of ten specialists with recognized expertise in forestry, natural resource management, environmental hazards, remote sensing, and geographic information systems (GIS) participated in the evaluation process. Experts were selected through purposive sampling based on their scientific qualifications, publication records, research experience in environmental risk and vulnerability assessment, and professional involvement in natural resource management.

The Delphi process was designed to derive consensus-based weights reflecting the relative importance of the selected environmental hazards. Consistent with established Delphi methodology, a relatively small expert panel was considered appropriate because the weighting procedure required highly specialized knowledge and focused evaluation of a limited number of variables (Miller, 2001). The level of agreement achieved during the initial assessment was sufficiently high, eliminating the need for additional consultation rounds (Landeta, 2006; Bederman et al., 2010). Participation was voluntary, responses were anonymized, and all experts were informed of the study objectives prior to completing the questionnaire.

The degree of expert consensus was evaluated using Cronbach's alpha coefficient, a widely applied measure of internal consistency and agreement among expert judgments. Cronbach's alpha was calculated as Eq. 4:

$$\alpha_x = k/k - 1(1 - \sum \sigma_{y_i}^2/\sigma_x^2) \quad (4)$$

where k represents the number of experts, $\sigma_{y_i}^2$ is the variance related to each response of each expert and σ_x^2 is the variance of the total responses for each expert. The coefficient ranges from 0 to 1, with higher values indicating stronger agreement among experts. The calculated Cronbach's alpha value of 0.91 demonstrated a very high level of consensus, confirming the reliability of the elicited judgments and supporting the use of a single Delphi round.

Following consensus assessment, the relative importance of each environmental hazard was determined using the weighting procedure proposed by Hasanzadeh et al. (2012). The method integrates the percentage

of importance assigned to each hazard with its corresponding importance level to derive a Normalized Importance Coefficient (NIC), which represents the final relative weight used in subsequent analyses. The NIC was calculated as Eq. 5:

$$\mathrm{NIC} = \frac{\mathrm{P}\times\mathrm{D}}{\sum(\mathrm{P}\times\mathrm{D})} \quad (5)$$

where NIC is the Normalized Importance Coefficient, P is the importance percentage, and D is the degree of importance for each variable.

The resulting weights were subsequently incorporated into the multi-hazard assessment framework to quantify the relative influence of individual environmental hazards on forest ecosystem resilience.

2.5. Development of the exposure index

To quantify the cumulative exposure of forest ecosystems to multiple environmental hazards, a composite Environmental Exposure Index (EI) was developed through a weighted linear combination approach (Mafi-Gholami et al., 2021). Prior to integration, each hazard layer was standardized and weighted according to the expert-derived importance coefficients obtained from the Delphi analysis. This procedure ensured that the contribution of each hazard reflected its relative influence within the overall multi-hazard framework.

The weighted hazard layers were subsequently integrated within the GIS environment to generate a spatially explicit exposure surface representing the combined effects of drought, SoVI, extreme temperature, high-speed wind, wildfire, flood, landslide, and dust hazards across the forest landscapes. The Environmental Exposure Index was calculated as Eq. 6:

$$\mathrm{EI} = \frac{So+D+T+W+WF+F+L+DT}{8} \quad (6)$$

where *EI* denotes the Environmental Exposure Index, So represents the social vulnerability index layer, *D* represents the weighted drought hazard layer, *T* the weighted maximum temperature hazard layer, *W* the weighted high-speed wind hazard layer, *WF* the weighted wildfire hazard layer, *F* the weighted flood hazard layer, *L* the weighted landslide hazard layer, and *DT* the weighted dust hazard layer.

The resulting index provides an integrated measure of the intensity and spatial distribution of environmental exposure, enabling the identification of forest areas subjected to cumulative multi-hazard pressures. For enhanced interpretation and spatial comparison, the EI map was classified into four exposure categories (low, moderate, high, and very high), thereby facilitating the assessment of exposure gradients and supporting subsequent vulnerability and resilience analyses.

2.6. Model validation

The predictive performance and spatial reliability of the EI were evaluated using three independent datasets representing major manifestations of environmental stress and ecosystem degradation within the Zagros

forests. These datasets consisted of 159 oak decline locations, 187 field-observed forest degradation sites, and 102 recorded wildfire hotspots. Because these ecological disturbances are widely recognized as key outcomes of cumulative environmental pressures in forest ecosystems, they provide an appropriate basis for independent model validation. A total of 448 validation points were employed in the assessment. Importantly, none of these observations were used during hazard mapping, weighting procedures, or index construction, ensuring a fully independent validation process. The geographic coordinates of all validation points were overlaid onto the final Environmental Exposure Index map, and their distribution across the exposure classes (very low, low, moderate, high, and very high) was extracted and analyzed. The validation framework was based on the premise that a robust exposure model should exhibit strong spatial correspondence between predicted high-exposure zones and independently observed ecological disturbance events. Accordingly, the frequency and cumulative percentage of validation points occurring within each exposure category were calculated to quantify the degree of spatial agreement between modeled exposure patterns and observed ecosystem impacts.

Model performance was assessed by examining the concentration of validation points within the high and very high exposure classes. A substantial accumulation of oak decline locations, degradation sites, and wildfire occurrences in these categories was interpreted as evidence of the model's ability to accurately identify environmentally stressed areas and delineate critical multi-hazard exposure hotspots. This independent observational validation approach provides an objective measure of model reliability and enables evaluation of the consistency between predicted exposure patterns and real-world manifestations of environmental degradation across the forest ecosystems.

2.7. Spatial analysis of environmental exposure across forest structural classes

To investigate the relationship between environmental exposure intensity and forest structural characteristics, a canopy-cover classification map of the study area was incorporated into the analysis. The dataset, provided by the General Directorate of Natural Resources and Watershed Management of Kohgiluyeh and Boyer-Ahmad Province, was produced in 2020 using Sentinel-2 satellite imagery, field observations, and expert interpretation conducted within the national forest monitoring framework. Forest stands were classified into five canopy-cover categories: 1–5%, 5–10%, 10–25%, 25–50%, and >50%. The classified Environmental Exposure Index (EI) map was spatially intersected with the forest canopy-cover classes to evaluate how exposure patterns vary across different levels of forest structural development. This spatial overlay enabled the quantification of the proportion of each canopy-cover class occurring within the four exposure categories (low, moderate, high, and very high).

The resulting distribution patterns were used to assess structural vulnerability across the forest landscape and to identify whether specific forest conditions are disproportionately exposed to cumulative

environmental hazards. By linking exposure intensity to canopy-cover gradients, the analysis provides insights into the spatial heterogeneity of environmental stress and highlights forest structural classes that may be more susceptible to the combined impacts of multiple environmental disturbances. This approach contributes to a more comprehensive understanding of the interactions between forest structure and multi-hazard exposure, thereby supporting ecosystem-based risk assessment and targeted forest management strategies.

3. Results

3.1. Spatial variability of environmental hazards across the forest ecosystems

The results reveal substantial heterogeneity in hazard intensity, highlighting the complex environmental conditions governing ecosystem exposure throughout the region (Table 2). Among the evaluated hazards, actual evapotranspiration exhibited pronounced spatial variation, reflecting marked differences in moisture availability and water-stress conditions across the forest landscapes. Similarly, the spatial distribution of maximum temperature indicated a clear thermal gradient, suggesting varying levels of heat stress that may influence ecosystem functioning and vegetation resilience. The observed patterns of drought and dust activity further demonstrate the widespread influence of aridification processes, with large portions of the study area exposed to elevated levels of climatic stress.

In contrast, high-speed wind displayed comparatively lower spatial variability, although localized areas remained subject to intensified wind-related disturbances. Landslide and flood susceptibility showed substantial variation across the region, indicating the coexistence of diverse geomorphological and hydrological conditions that may increase ecosystem sensitivity to environmental change. Wildfire hazard also exhibited considerable spatial differentiation, reflecting differences in fuel availability, climatic conditions, and landscape characteristics among forest stands. The SoVI revealed notable spatial disparities in the capacity of local communities to cope with environmental disturbances. Areas characterized by high social vulnerability frequently coincided with elevated levels of environmental stress, suggesting the presence of coupled socio-ecological risks within portions of the forest landscape.

Table 2. Intensity of multiple environmental hazards in study forest area

Hazard	Category			
	Low	Moderate	High	Very high
Evapotranspiration (mm)	<417.1	417.2-491.8	491.8-567.9	567.9<
Maximum temperature	<0.0174	0.0174-0.0197	0.0197-0.0222	0.0222<
SoVI	<0.355	0.355-0.671	0.671-0.834	0.834<
Dust storm	<0.381	0.381-0.584	0.584-0.761	0.761<
Drought	<67.6	67.6-74.1	74.1-81.2	81.2<
High-speed winds	<0.00105	0.00105-0.00114	0.00114-0.00124	0.00124<
Landslide	<680	680-880	880-1018	1018<
Flood	<0.586	0.586-0.780	0.780-0.980	0.980<
Wildfire	<0.391	0.391-0.535	0.535-0.670	0.670<

3.2. Relative weights of environmental hazards

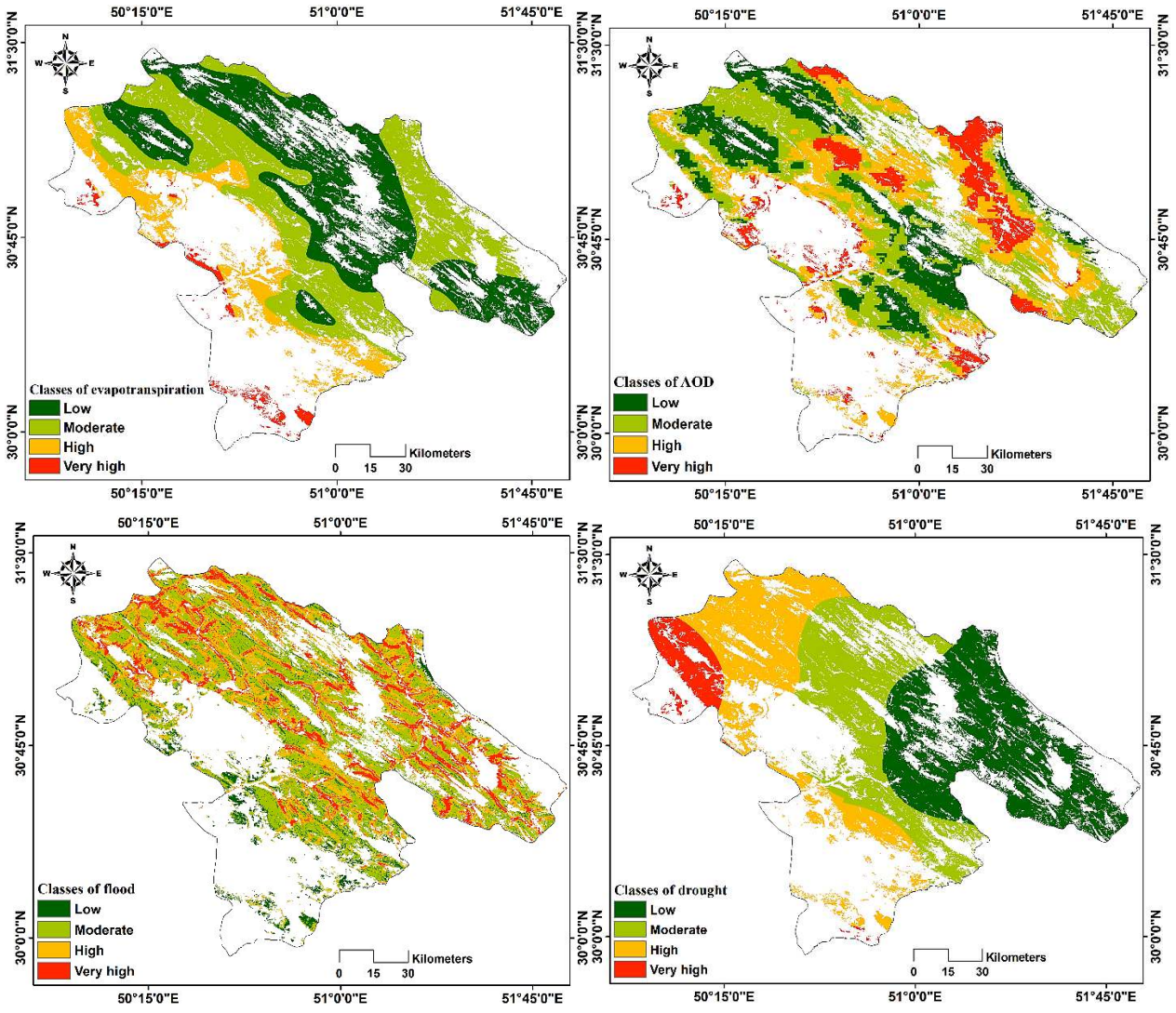
The Delphi-based expert elicitation process revealed differences in the perceived importance of the environmental hazards considered in the exposure assessment framework (Table X). According to the expert panel, drought received the highest relative weight (0.147), indicating the strongest consensus regarding its importance within the study area. Fire hazard (0.133) and social vulnerability (0.128) ranked second and third, respectively. Dust storms (0.121) and maximum temperature (0.114) were also assigned relatively high weights, reflecting their perceived influence on environmental pressures affecting forest ecosystems. The remaining hazards received comparatively lower weights, including landslides (0.101), floods (0.094), high-speed winds (0.086), and evapotranspiration (0.076). These weights represent the collective judgment of the participating experts regarding the relative contribution of each hazard to the exposure component of vulnerability and were subsequently used in the weighted overlay analysis for constructing the multi-hazard exposure index.

3.3. Spatial distribution of environmental hazards

The classified hazard maps revealed substantial spatial heterogeneity in the distribution of environmental hazards across the forest ecosystems of Kohgiluyeh and Boyer-Ahmad Province (Fig. 2). Distinct spatial patterns were observed among the investigated hazards. Climatic hazards, particularly drought, maximum temperature, dust storms, and evapotranspiration, exhibited relatively broad spatial extents, with moderate to high hazard classes covering large portions of the forested landscape. In contrast, flood and landslide hazards displayed more localized distributions and were primarily concentrated within specific topographic settings.

The spatial patterns of wildfire hazard and high-speed winds were characterized by the occurrence of discrete hotspots distributed across particular forest sub-regions. Furthermore, several areas exhibited

spatial overlap among multiple hazards, indicating the presence of zones simultaneously exposed to different environmental stressors. The resulting hazard maps demonstrate that the spatial distribution of environmental threats is neither uniform nor independent, but rather varies considerably across the study area, producing distinct gradients of environmental exposure within the Zagros forest ecosystems (Fig. 2).



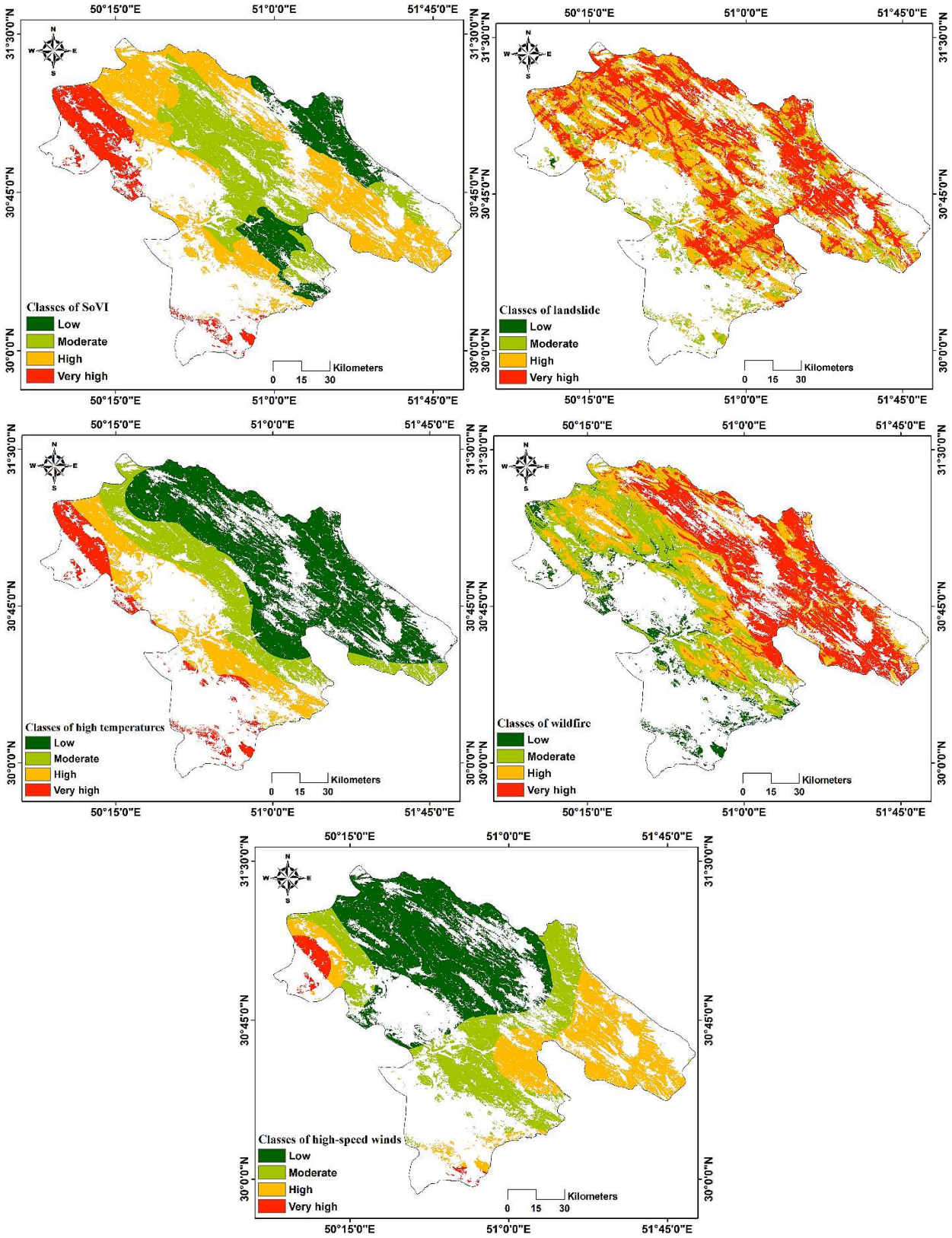


Fig. 2. The classification of multiple hazard maps affecting forest areas

3.3. Spatial pattern of the multi-hazard exposure index

The final exposure map revealed a pronounced spatial heterogeneity in the distribution of multi-hazard exposure across the forest ecosystems of Kohgiluyeh and Boyer-Ahmad Province (Fig. 3). Areas classified within the low exposure category were primarily concentrated in the central parts of the study area and in several mountainous forest regions. In contrast, moderate and high exposure classes occupied extensive portions of the landscape and formed relatively continuous spatial belts across different forested zones.

The very high exposure class exhibited a more clustered distribution and was mainly concentrated in the western and southern parts of the province, with additional localized patches occurring in eastern forest areas. These zones represent areas where elevated levels of multiple environmental hazards spatially coincide. Overall, the exposure map demonstrates substantial spatial variability in the intensity of environmental hazard exposure, indicating that forest ecosystems within the study area are subjected to markedly different levels of environmental stress and disturbance pressure (Fig. 3).

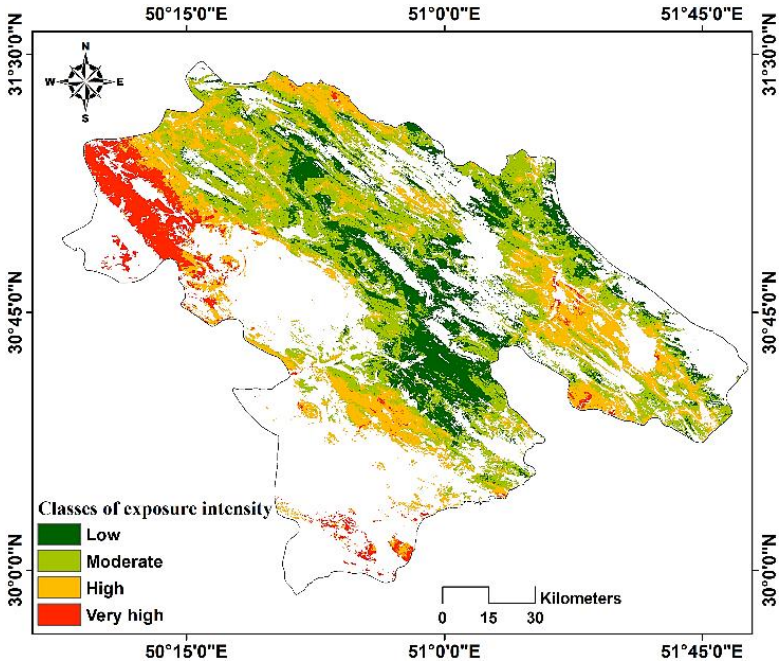


Fig. 3. The spatial changes of the intensity of environmental hazard exposure in forest areas of Kohgiluyeh and Boyer-Ahmad Province.

3.4. Validation of the multi-hazard exposure model

The independent validation analysis revealed a strong spatial correspondence between the modeled exposure classes and the distribution of observed ecological disturbance indicators. Of the 448 validation points, comprising 159 oak decline locations, 187 field-observed forest degradation sites, and 102 recorded wildfire hotspots, 45% were located within the *very high* exposure class and 30% within the *high* exposure class.

Consequently, 75% of all validation points occurred in areas identified by the model as having high to very high levels of exposure to environmental hazards. In comparison, 10% of the validation points were associated with the *moderate* exposure class, whereas only 8% and 7% occurred within the *low* and *very low* exposure classes, respectively. The pronounced concentration of validation points in the upper exposure categories indicates a clear spatial association between modeled exposure levels and independently observed manifestations of forest stress and disturbance. These results demonstrate that locations affected by oak decline, forest degradation, and wildfire occurrence are disproportionately distributed within areas characterized by elevated environmental exposure. The relatively limited proportion of validation points found in the low and very low exposure classes further supports the ability of the model to discriminate between areas with contrasting levels of environmental pressure. Overall, the validation results indicate that the proposed exposure model effectively captures the spatial distribution of environmental hazard exposure across the Zagros forest ecosystems and successfully identifies areas subjected to higher levels of environmental stress.

3.5. Spatial variations in multi-hazard exposure across forest canopy density classes

The spatial distribution of the exposure index across different forest canopy density classes revealed a clear relationship between forest structure and the intensity of environmental hazard exposure (Figs. 4 and 5). Distinct spatial differences were observed among canopy density classes, with low-density forests generally exhibiting a greater extent of high and very high exposure zones, whereas areas characterized by denser canopy cover were dominated by lower exposure levels.

The percentage composition of exposure classes further highlighted these differences. Within the lowest canopy density class (1–5%), moderate exposure represented the largest proportion of the area (41.2%), followed by low exposure (20.1%). High and very high exposure classes accounted for 30.2% and 8.5% of the area, respectively. In contrast, forests with canopy densities between 25% and 50% exhibited the highest proportion of moderate exposure (45.6%) and the lowest proportion of very high exposure (5.9%).

Intermediate canopy density classes displayed transitional characteristics. In forests with canopy cover ranging from 10% to 25%, moderate exposure remained dominant (42.6%), while the proportion of high exposure increased to 28.2%. Moreover, the share of very high exposure gradually increased as canopy density declined, reaching 9.5% and 11.5% in the lower-density forest classes, accompanied by a corresponding reduction in the proportion of moderate exposure (41.5% and 40.7%, respectively).

Overall, the results indicate a systematic shift in the distribution of exposure classes across the forest structural gradient. High and very high exposure categories occupied larger proportions of low-density forest areas, whereas moderate and low exposure classes were more prevalent in forests characterized by greater canopy cover (Figs. 4 and 5).

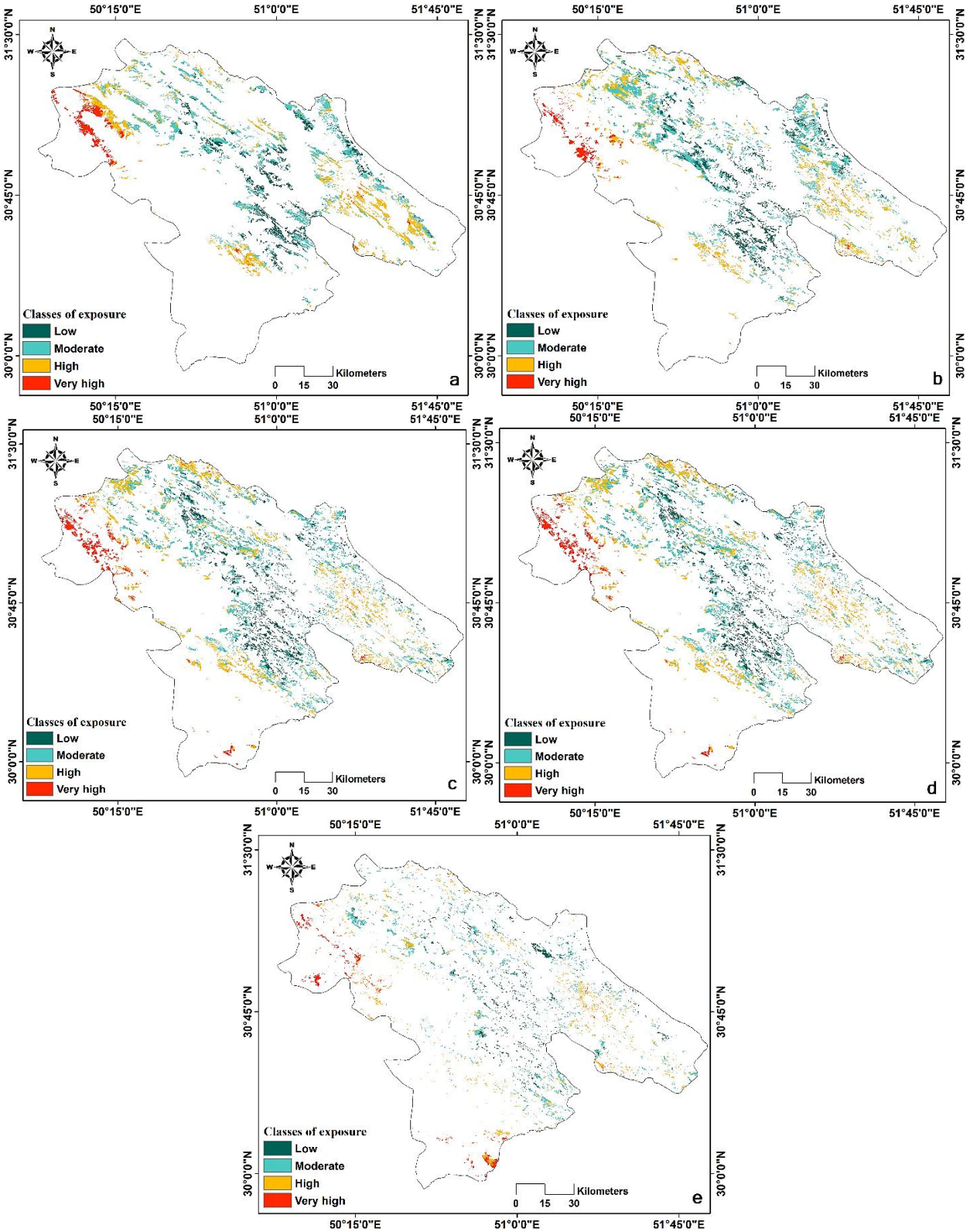


Fig. 4. The distribution of the intensity of exposure to multiple hazards within each of forest density classes (a: density 1-5%, b: 5-10%, c: 10-25%, d: 25-50%, and e: 50%<).

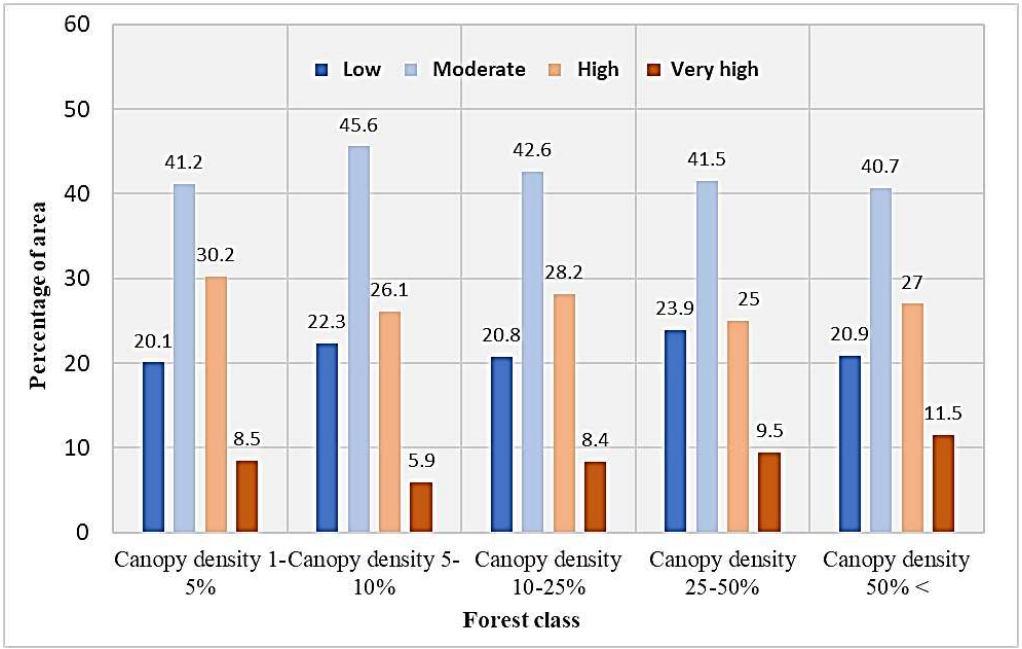


Fig. 5. The percentage of forest density area within the four categories of multiple hazard occurrence intensity in the study forests.

4. Discussion

Understanding the spatial distribution of exposure to multiple environmental hazards represents a fundamental prerequisite for comprehensive forest vulnerability assessments and for developing risk-informed management strategies under accelerating environmental change. By integrating diverse climatic, ecological, geomorphological, and socio-environmental stressors into a unified analytical framework, exposure mapping provides critical insights into where and to what extent forest ecosystems are subjected to cumulative environmental pressures. Such information is indispensable for identifying ecological hotspots, prioritizing conservation interventions, and enhancing the long-term resilience of forest landscapes (Mafi-Gholami et al., 2021; Pirasteh et al., 2024).

In the present study, the exposure component of vulnerability was spatially modeled across the forest ecosystems of Kohgiluyeh and Boyer-Ahmad Province through the integration of nine major environmental hazards, including drought, evapotranspiration, wildfire, extreme wind, maximum temperature, flood, landslide, dust storms, and social vulnerability. To account for differences in the relative importance of individual hazards, a Delphi-based expert elicitation approach was employed. The results indicated a clear dominance of climate-related hazards in shaping the overall exposure pattern. Drought received the highest expert-assigned weight, followed by wildfire and social vulnerability, whereas dust storms and maximum temperature were also identified as influential contributors. It should be emphasized that these weights represent expert judgments regarding the relative importance of hazards within the study system and should

not be interpreted as direct empirical estimates of the actual contribution of each hazard to ecological degradation.

The prominence of drought is consistent with a growing body of evidence identifying prolonged moisture deficits as one of the principal drivers of forest degradation throughout the Zagros region (Jaafari et al., 2017, 2022; Mahmoudi et al., 2023). Recurrent drought events have been linked to reduced physiological performance, declining growth rates, weakened regeneration capacity, increased susceptibility to pests and pathogens, and widespread oak decline (Goodarzi et al., 2019; Attarod et al., 2025). Moreover, drought rarely acts in isolation. Instead, it frequently interacts with elevated temperatures, dust deposition, and wildfire occurrence, producing cascading ecological impacts that amplify ecosystem stress and accelerate degradation processes (Jaafari et al., 2026). The relatively high ranking of wildfire further reflects the increasing importance of fire disturbances under warmer and drier climatic conditions, while the contribution of social vulnerability highlights the importance of human dimensions in shaping forest exposure patterns and management effectiveness.

The resulting exposure map revealed a markedly heterogeneous spatial pattern across the study area. Extensive portions of the western, southern, and localized eastern forest landscapes were classified as high or very high exposure zones, whereas lower exposure levels were generally concentrated within central mountainous areas characterized by denser forest cover and comparatively favorable environmental conditions. Such spatial heterogeneity highlights the uneven distribution of environmental pressures across the Zagros forests and suggests that future conservation efforts should be spatially prioritized rather than uniformly implemented (Haidari et al., 2025).

One of the most important findings of this study is the strong association between forest canopy structure and exposure intensity. Forest stands characterized by sparse canopy cover exhibited substantially higher proportions of high and very high exposure classes, whereas denser forests were predominantly associated with low to moderate exposure levels. Similar relationships between forest structural degradation and increasing environmental vulnerability have been reported in mountain forest ecosystems worldwide (Pirasteh et al., 2024; Valavi et al., 2019).

This pattern is ecologically meaningful and can be explained through several interconnected biophysical and hydrological mechanisms. First, canopy cover functions as a critical regulator of forest microclimate. Dense canopies reduce incoming solar radiation, moderate surface temperatures, decrease soil evaporation, and maintain higher moisture availability within the forest floor. Conversely, canopy degradation increases direct solar exposure and accelerates soil moisture depletion, thereby intensifying drought stress and thermal extremes. These effects are particularly pronounced in the semi-arid climatic conditions of the Zagros Mountains, where water availability already represents a major limiting factor for ecosystem functioning (Attarod et al., 2025).

Second, forest canopies play a fundamental role in hydrological regulation. Reduced canopy density diminishes rainfall interception capacity, lowers infiltration rates, and increases surface runoff generation. Simultaneously, declining tree density is often accompanied by reductions in root biomass and rooting depth, weakening soil cohesion and slope stabilization processes. Consequently, sparsely forested landscapes become increasingly susceptible to soil erosion, flash floods, and landslide occurrence. Numerous studies have demonstrated that intact forest cover substantially enhances watershed stability and mitigates geomorphological hazards through both hydrological and mechanical reinforcement mechanisms (Liu et al., 2013; Thakur et al., 2021).

Third, low-density forests frequently exhibit discontinuous vegetation cover, greater accumulation of dry biomass, and warmer and drier microclimatic conditions, all of which increase wildfire susceptibility. Under such circumstances, drought, heat stress, and fire interact through positive feedback mechanisms, creating self-reinforcing degradation pathways (Jaafari et al., 2022). Therefore, the observed concentration of high exposure values within canopy-cover classes below 10% should not be interpreted merely as a spatial correlation. Rather, it reflects a broader decline in the ecological buffering capacity, self-regulation potential, and adaptive resilience of degraded forest ecosystems.

The implications of these findings become even more significant when considered within the context of projected climate change. Climate projections for the Middle East and the Zagros region consistently indicate increasing temperatures, declining precipitation, more frequent drought episodes, and heightened climatic variability during the coming decades (Etemadi et al., 2016). Such trends are likely to expand both the spatial extent and intensity of environmental exposure across forest ecosystems, including currently less affected stands. Simultaneously, recent studies suggest that climate change may increase the frequency and magnitude of extreme precipitation events, thereby elevating flood and erosion risks in steep mountainous landscapes (Forzieri et al., 2022). The overlap observed between densely forested northern and eastern regions and areas characterized by elevated flood susceptibility indicates that future environmental change may alter the current spatial configuration of vulnerability and generate new ecological risk hotspots.

From a management perspective, the identified high-exposure zones should be prioritized for targeted intervention. Adaptive forest management strategies should focus on drought mitigation, wildfire prevention, restoration of degraded stands, enhancement of natural regeneration, watershed rehabilitation, soil and water conservation measures, and the maintenance of structural forest complexity (Chirwa et al., 2026). Increasing canopy density and improving ecosystem integrity may simultaneously reduce exposure to multiple interacting hazards while strengthening overall ecosystem resilience.

Despite the robustness of the proposed framework, several limitations should be acknowledged. The spatial representation of climatic hazards was constrained by the limited number of long-term meteorological stations available within and around the forest ecosystems. In addition, uncertainties associated with

remotely sensed datasets, spatial interpolation procedures, and expert-based weighting may influence the final exposure estimates. Furthermore, the current framework did not explicitly incorporate emerging ecological stressors such as forest pests, pathogens, and oak decline dynamics, which are increasingly recognized as important drivers of ecosystem degradation in the Zagros forests (Goodarzi et al., 2019).

Future research should therefore focus on integrating high-resolution remote sensing products, long-term ecological monitoring data, climate change scenarios, and biotic disturbance indicators into multi-hazard vulnerability assessments. In particular, incorporating spatially explicit maps of pest outbreaks, disease prevalence, and oak decline processes derived from Sentinel-2, Landsat, and field-based monitoring programs would substantially improve the comprehensiveness and predictive capability of future vulnerability models. Such advancements would contribute to the development of more effective ecosystem-based adaptation strategies and strengthen the scientific basis for sustainable forest management under rapidly changing environmental conditions.

5. Limitations, management implications, and future research directions

Although the present study provides one of the first spatially explicit assessments of multi-hazard exposure across the Zagros forest ecosystems through the simultaneous integration of nine environmental and socio-environmental hazards, the findings should be interpreted in light of several limitations.

First, the spatial characterization of climatic hazards was constrained by the limited density and distribution of long-term meteorological stations within and adjacent to the forest landscapes. Consequently, part of the climatic information was derived through spatial interpolation and reanalysis-based datasets, which inevitably introduce a degree of uncertainty into the resulting hazard surfaces. Second, several hazard layers were generated from remotely sensed products whose accuracy may be influenced by spatial and temporal resolution, classification performance, sensor limitations, and environmental conditions. Third, hazard weighting was conducted using a Delphi-based expert elicitation framework. Therefore, the assigned weights represent the relative importance of hazards according to expert knowledge and consensus rather than direct empirical measurements of their actual contribution to ecosystem degradation processes. Finally, environmental hazards are inherently dynamic and non-stationary; thus, the exposure patterns identified in this study reflect the environmental conditions of the investigated period and may evolve under future climatic, ecological, and socio-economic changes.

Despite these limitations, the findings provide important insights for the sustainable management and conservation of the Zagros forests. The identification of high- and very high-exposure hotspots offers a scientifically robust basis for prioritizing conservation actions, allocating limited financial and institutional resources, and targeting restoration interventions where ecological risks are greatest. Particularly noteworthy is the concentration of critical exposure zones within sparse and moderately degraded forest

stands, highlighting the importance of forest structure as a key determinant of ecosystem resilience. Consequently, management efforts aimed at enhancing canopy density, restoring degraded landscapes, controlling overgrazing, reducing fuel loads, mitigating wildfire risk, and strengthening community-based forest stewardship are likely to generate substantial co-benefits by simultaneously reducing exposure to multiple interacting hazards. Furthermore, the exposure maps developed in this study can serve as an operational decision-support tool for watershed management planning, forest conservation programs, ecological restoration initiatives, and climate adaptation strategies throughout the Zagros region.

Future research should focus on advancing multi-hazard vulnerability assessments through the integration of higher-resolution geospatial datasets, expanded ecological monitoring networks, and long-term climatic observations. Incorporating the remaining dimensions of vulnerability, namely sensitivity and adaptive capacity, alongside exposure would facilitate the development of a more comprehensive and policy-relevant vulnerability framework for forest ecosystems. In addition, future studies should explicitly address the temporal dynamics of environmental hazards, evaluate alternative climate change scenarios, and investigate cumulative, cascading, and synergistic interactions among multiple stressors. Particular attention should also be given to emerging ecological threats such as pest outbreaks, forest diseases, and oak decline phenomena, which are increasingly shaping the future trajectory of Zagros forest ecosystems. Such efforts will improve predictive capability, reduce uncertainty in vulnerability assessments, and strengthen the scientific foundation for ecosystem-based adaptation and resilience-building strategies under a rapidly changing climate.

6. Conclusions

This study developed a spatially explicit multi-hazard exposure assessment framework to evaluate the distribution and intensity of environmental pressures across the forest ecosystems of Kohgiluyeh and Boyer-Ahmad Province, one of the most ecologically significant sectors of the Zagros Mountains. By integrating nine environmental and socio-environmental hazards within a GIS-based analytical framework, the study revealed a pronounced spatial heterogeneity in exposure patterns and identified extensive forest areas that are currently subjected to high and very high levels of cumulative environmental stress. The findings demonstrate that climate-related hazards, particularly drought, together with wildfire and social vulnerability, constitute the dominant drivers shaping the spatial configuration of exposure across the study area. Independent validation using observed oak decline locations, forest degradation sites, and recorded wildfire hotspots further confirmed the ability of the proposed framework to reliably identify environmentally stressed and ecologically vulnerable landscapes. Moreover, the results revealed a clear and systematic relationship between forest canopy structure and exposure intensity, whereby sparsely forested stands consistently exhibited higher levels of environmental exposure than denser forest ecosystems.

Beyond documenting current hazard patterns, the study provides important evidence that forest structural degradation may amplify exposure to multiple environmental stressors through interconnected ecological, hydrological, and microclimatic mechanisms. These findings underscore the critical role of maintaining forest integrity and canopy cover in enhancing ecosystem resilience under increasing environmental pressures. From a practical perspective, the generated exposure maps offer a valuable decision-support resource for identifying priority intervention areas, optimizing conservation investments, guiding restoration programs, and supporting climate adaptation planning. More broadly, the proposed framework contributes to the transition from conventional single-hazard approaches toward integrated multi-hazard risk assessment in forest ecosystems. Given the accelerating impacts of climate change across the Middle East and the Zagros Mountains, such integrated approaches will be essential for strengthening ecosystem resilience, reducing environmental vulnerability, and ensuring the long-term sustainability of one of the most important forest landscapes in Southwest Asia.

Funding

No funding was received for conducting this study.

Author Contributions Statement

D.M.: Conceptualization, Data curation, Methodology, Software, Formal analysis, Validation, Investigation, Writing – original draft. **A.J.:** Data curation, Methodology, Software, Validation, Visualization, Writing – review & editing. **B.T.P.:** Conceptualization, Methodology, Supervision, Project administration, Writing – review & editing.

Ethics declarations

Ethics approval

All authors have read, understood, and have complied as applicable with the statement on “Ethical responsibilities of Authors” as found in the “Instructions for Authors.”

Competing interests

The authors declare no competing interests.

Data availability

The data will be made available on request.

References

Abdollahi, K., Bashir, I., Verbeiren, B., Harouna, M. R., Van Griensven, A., Huysmans, M., & Batelaan, O. (2017). A distributed monthly water balance model: Formulation and application on Black Volta Basin. *Environmental Earth Sciences, 76*, 198. https://doi.org/10.1007/s12665-017-6512-1

Adger, W. N. (2006). Vulnerability. *Global Environmental Change, 16*(3), 268–281. https://doi.org/10.1016/j.gloenvcha.2006.02.006

Attarod, P., Zhu, H., Beiranvand, S., Pypker, T. G., Bayramzadeh, V., Soofi Mariv, H., & Karimi, K. (2025). Past and future climate change in the Zagros region of western Iran. *Anthropocene, 50*, 100475. https://doi.org/10.1016/j.ancene.2025.100475

Beiranvand, S., Bayramzadeh, V., Attarod, P., Pourtahmasi, K., & Nadi, M. (2024). Increasing drought frequency in the central Zagros Mountains of western Iran over the past two centuries. *Journal of Arid Environments, 224*, 105240. https://doi.org/10.1016/j.jaridenv.2024.105240

Chirwa, P. W., & Makhubele, L. (2026). Forest landscape restoration governance and management in sub-Saharan Africa: what are the implications for the implementation of Forest Landscape Restoration programmes?. *International Forestry Review*, *28*(2), 115-128. https://doi.org/10.1505/146554826841270511

Donmez, C., & Berberoglu, S. (2016). A comparative assessment of catchment runoff generation and forest productivity in a semi-arid environment. *International Journal of Digital Earth, 9*(10), 942–962. https://doi.org/10.1080/17538947.2016.1158875

Ellison, A. M. (2000). Mangrove restoration: Do we know enough? *Restoration Ecology, 8*(3), 219–229. https://doi.org/10.1046/j.1526-100x.2000.80033.x

Eslami-Andargoli, L., Dale, P. E. R., Sipe, N., & Chaseling, J. (2009). Mangrove expansion and rainfall patterns in Moreton Bay, southeast Queensland, Australia. *Estuarine, Coastal and Shelf Science, 85*(2), 292–298. https://doi.org/10.1016/j.ecss.2009.08.011

Etemadi, H., Samadi, S. Z., Sharifikia, M., & Smoak, J. M. (2016). Assessment of climate change downscaling and non-stationarity on the spatial pattern of a mangrove ecosystem in an arid coastal region of southern Iran. *Theoretical and Applied Climatology, 126*, 35–49. https://doi.org/10.1007/s00704-015-1552-5

FAO. (2020). *Global forest resources assessment 2020: Main report*. Food and Agriculture Organization of the United Nations. https://openknowledge.fao.org/server/api/core/bitstreams/9f24d451-2e56-4ae2-8a4a-1bc511f5e60e/content

Forzieri, G., Dakos, V., McDowell, N. G., Alkama, R., & Cescatti, A. (2022). Emerging signals of declining forest resilience under climate change. *Nature, 608*(7923), 534–539. https://doi.org/10.1038/s41586-022-04959-9

Goodarzi, M., Pourhashemi, M., & Azizi, Z. (2019). Investigation on Zagros forests cover changes under the recent droughts using satellite imagery. *Journal of Forest Science, 65*(1), 9–17. https://doi.org/10.17221/61/2018-JFS

Haidari, M., Goujani, H. J., Maleki, S., Jaafari, A., Pourhashemi, M., Henarah, J., ... & Khanhasani, M. (2025). Oak decline in the Zagros Forests: Temporal variation, severity, and environmental and stand structural drivers. *Global Ecology and Conservation*, e03811. https://doi.org/10.1016/j.gecco.2025.e03811

Jaafari, A., & Mafi-Gholami, D. & Zenner, E. K. (2017). A Bayesian modeling of wildfire probability in the Zagros Mountains, Iran. *Ecological Informatics, 39*, 32–44. https://doi.org/10.1016/j.ecoinf.2017.03.003

Jaafari, A., Negahdarsaber, M., & Bordbar, S. K. (2026). Explainable wildfire susceptibility assessment using fuzzy-evolutionary rules and Monte Carlo sensitivity analysis. *Ecological Informatics*, 103878. https://doi.org/10.1016/j.ecoinf.2026.103878

Jaafari, A., Rahmati, O., Zenner, E. K., & Mafi-Gholami, D. (2022). Anthropogenic activities amplify wildfire occurrence in the Zagros eco-region of western Iran. Natural Hazards, 114(1), 457-473. https://doi.org/10.1007/s11069-022-05397-6

Khosravi, K., Panahi, M., Golkarian, A., Keesstra, S. D., Saco, P. M., Bui, D. T., & Lee, S. (2020). Convolutional neural network approach for spatial prediction of flood hazard at national scale of Iran. *Journal of Hydrology, 591*, 125552. https://doi.org/10.1016/j.jhydrol.2020.125552

Koks, E. E., Jongman, B., Husby, T. G., & Botzen, W. J. W. (2015). Combining hazard, exposure and social vulnerability to provide lessons for flood risk management. *Environmental Science & Policy, 47*, 42–52. https://doi.org/10.1016/j.envsci.2014.10.013

Leberger, R., Rosa, I. M., Guerra, C. A., Wolf, F., & Pereira, H. M. (2020). Global patterns of forest loss across IUCN categories of protected areas. *Biological Conservation, 241*, 108299. https://doi.org/10.1016/j.biocon.2019.108299

Li, J., & van de Lindt, J. W. (2025). Climate adaptation matrix concept for multidisciplinary community resilience in a changing climate. Natural Hazards Review, 26(2), 04025007. https://doi.org/10.1061/NHREFO.NHENG-2122

Liu, H., Williams, A. P., Allen, C. D., Guo, D., Wu, X., Anenkhonov, O. A., & Badmaeva, N. K. (2013). Rapid warming accelerates tree growth decline in semi-arid forests of Inner Asia. *Global Change Biology, 19*(8), 2500–2510. https://doi.org/10.1111/gcb.12217

Macek, M., Kopecký, M., & Wild, J. (2019). Maximum air temperature controlled by landscape topography affects plant species composition in temperate forests. *Landscape Ecology, 34*, 2541–2556. https://doi.org/10.1007/s10980-019-00903-x

Mafi-Gholami, D., Pirasteh, S., Ellison, J. C., & Jaafari, A. (2021). Fuzzy-based vulnerability assessment of coupled social-ecological systems to multiple environmental hazards and climate change. *Journal of Environmental Management, 299*, 113573. https://doi.org/10.1016/j.jenvman.2021.113573

Mahmoudi, B., Zenner, E., Mafi-Gholami, D., & Eshaghi, F. (2023). Livelihood analysis and a new inferential model for development of forest-dependent rural communities. *Sustainability, 15*(11), 9008. https://doi.org/10.3390/su15119008

Michelsen, O., McDevitt, J. E., & Coelho, C. R. (2014). A comparison of three methods to assess land use impacts on biodiversity in forestry plantations in New Zealand. *The International Journal of Life Cycle Assessment, 19*, 1214–1225. https://doi.org/10.1007/s11367-014-0742-1

Ngo, P. T. T., Panahi, M., Khosravi, K., Ghorbanzadeh, O., Kariminejad, N., Cerda, A., & Lee, S. (2021). Evaluation of deep learning algorithms for national scale landslide susceptibility mapping of Iran. *Geoscience Frontiers, 12*(2), 505–519. https://doi.org/10.1016/j.gsf.2020.06.013

Nguyen, K. A., Liou, Y. A., & Terry, J. P. (2019). Vulnerability of Vietnam to typhoons: A spatial assessment based on hazards, exposure and adaptive capacity. *Science of the Total Environment, 682*, 31–46. https://doi.org/10.1016/j.scitotenv.2019.04.069

Pirasteh, S., Fang, Y., Mafi-Gholami, D., Abulibdeh, A., Nouri-Kamari, A., & Khonsari, N. (2024). Enhancing vulnerability assessment through spatially explicit modeling of mountain social-ecological systems exposed to multiple environmental hazards. *Science of the Total Environment, 930*, 172744. https://doi.org/10.1016/j.scitotenv.2024.172744

Pourhashemi, M., Mohajer, M. R. M., Zobeiri, M., Amiri, G. Z., & Panahi, P. (2004). Identification of forest vegetation units in support of government management objectives in Zagros forests, Iran. *Scandinavian Journal of Forest Research, 19*(S4), 72–77. https://doi.org/10.1080/14004080410034083

Pouyan, S., Pourghasemi, H. R., Bordbar, M., Rahmanian, S., & Clague, J. J. (2021). A multi-hazard map-based assessment of flooding, gully erosion, forest fires, and earthquakes in Iran. *Scientific Reports, 11*(1), 14889. https://doi.org/10.1038/s41598-021-94266-6

Reckien, D. (2018). What is in an index? Construction method, data metric, and weighting scheme determine the outcome of composite social vulnerability indices in New York City. *Regional Environmental Change, 18*(5), 1439–1451. https://doi.org/10.1007/s10113-017-1273-7

Spehn, E. M., Rudmann-Maurer, K., & Körner, C. (2011). Mountain biodiversity. *Plant Ecology & Diversity, 4*(4), 301–302. https://doi.org/10.1080/17550874.2012.698660

Su, S., Pi, J., Wan, C., Li, H., Xiao, R., & Li, B. (2015). Categorizing social vulnerability patterns in Chinese coastal cities. *Ocean & Coastal Management, 116*, 1–8. https://doi.org/10.1016/j.ocecoaman.2015.06.026

885 Thakur, S., Negi, V. S., Dhyani, R., Satish, K. V., & Bhatt, I. D. (2021). Vulnerability assessments of
886 mountain forest ecosystems: A global synthesis. *Trees, Forests and People, 6*, 100156.
887 https://doi.org/10.1016/j.tfp.2021.100156
888 Valavi, R., Shafizadeh-Moghadam, H., Matkan, A., Shakiba, A., Mirbagheri, B., & Kia, S. H. (2019).
889 Modelling climate change effects on Zagros forests in Iran using individual and ensemble forecasting
890 approaches. *Theoretical and Applied Climatology, 137*, 1015–1025. https://doi.org/10.1007/s00704-018-
891 2625-z
892 Xia, M., Jia, K., Zhao, W., Liu, S., Wei, X., & Wang, B. (2021). Spatio-temporal changes of ecological
893 vulnerability across the Qinghai–Tibetan Plateau. *Ecological Indicators, 123*, 107274.
894 https://doi.org/10.1016/j.ecolind.2020.107274
895 Xiao, J., Sun, G., Chen, J., Chen, H., Chen, S., Dong, G., & Zhou, J. (2013). Carbon fluxes,
896 evapotranspiration, and water use efficiency of terrestrial ecosystems in China. *Agricultural and Forest*
897 *Meteorology, 182*, 76–90. https://doi.org/10.1016/j.agrformet.2013.08.007